THE JOURNAL OF PHYSICAL CHEMISTRY B

Article

pubs.acs.org/JPCB

Electron Transfer Mechanism in Organometallic Molecules Studied by Subpicosecond Extended X-ray Absorption Fine Structure Spectroscopy

Wei-Kan Chen,[†] Jie Chen,*[,‡] and Peter M. Rentzepis*[,†]

[†]Department of Chemistry, University of California at Irvine, California 92697, United States

[‡]Key Laboratory for Laser Plasmas (Ministry of Education) and Department of Physics, Shanghai Jiao Tong University, Shanghai 200240, China

ABSTRACT: The mechanism responsible for the redox reaction of $[Co^{III}(en)_3]Ac_3$ to Co(II) complex has been determined to be intramolecular electron transfer. It was measured in real time by means of subpicosecond extended X-ray absorption fine structure spectra, EXAFS, and optical experiments and supported by density functional theory calculations. The proposed mechanism is based on histograms of bond length changes of the transient structures measured as a function of time, with subpicosecond time and sub-Angstrom resolution and femtosecond transient spectra and kinetics after excitation with a 267 nm femtosecond pulse. Even though four Fe and Co complexes were excited in the charge transfer band and the photoinduced redox reaction proceeds with similar high redox quantum yield, the dominant electron operating mechanism differs: intramolecular for amine metal complexes and intermolecular for oxalate metal complexes. The ligand orientation degree of freedom and counterion effect are proposed to provide tentative explanation for the electron transfer mechanism.

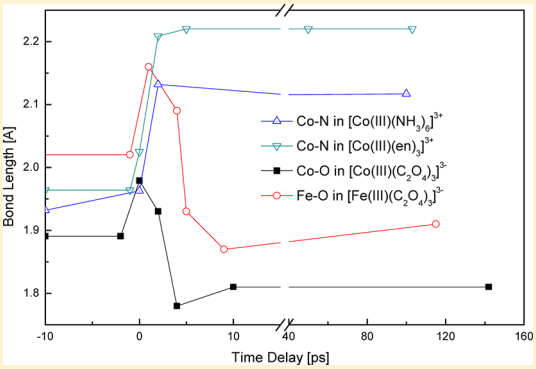

1. INTRODUCTION

Electron transfer (ET) is a widely occurring process in nature that has been investigated theoretically and experimentally for decades in chemical and biological molecules.[1−7] Among the large number of molecules that have been studied, cobalt, iron, copper, and ruthenium complexes are probably the ones most often used as models for electron transfer.[8−14] The mechanism that governs ET is, usually, either intermolecular that occurs in the hundreds of picoseconds to millisecond range limited to a large extend by the diffusion rate of the donor and acceptor groups or intramolecular controlled by the time needed for an electron to travel from the donor atom (group) to the acceptor when both are located within the same redox molecule. Intramolecular ET lifetimes may vary from femtoseconds to picoseconds in small molecules and orders of magnitude longer in large biological molecules.[7,15]

In many cases it is difficult to predict accurately whether the mechanism is inter- or intramolecular, or to measure the rate of electron transfer within a molecule because of the high ET rate. However, the development of time-resolved optical spectroscopy and lately ultrafast X-ray diffraction and X-ray absorption techniques have provided a powerful means for the detection of ultrafast transient excited states and intermediate species evolved during the course of electron transfer processes in chemical[16,17] and biological[18,19] molecules.[20−28] The redox reactions of several iron and cobalt complexes have been studied by optical spectroscopy, and lately the electron transfer rate and mechanism of those complexes have been determined after 267 nm femtosecond pulse excitation in the ligand to metal charge transfer (LMCT) band.[29−32] Under these excitation conditions it would be expected that the redox reaction would follow an intramolecular ET mechanism, where an electron is transferred, directly, from the ligand to the metal within a few picoseconds. However, recent ultrafast time-resolved optical and extended X-ray absorption fine structure (EXAFS) experimental results indicate that for some Co(III) and Fe(III) oxalate complexes the electron transfer process is governed by an intermolecular rather than intramolecular mechanism. Therefore, one might question what these results imply and if one must assume that all photoinduced iron and cobalt coordination compounds and even other metal−organic ligand redox reactions proceed via intermolecular electron transfer. However, recent time-resolved EXAFS data and theoretical calculation revealed that excitation of the $[Co^{III}(NH_3)_6]^{3+}$ complex into the charge transfer (CT) band leads to direct intramolecular electron transfer.[33] These studies also suggest that it is rather difficult to predict, a priori, the ET mechanism even if the charge transfer takes place within one molecule and when the excitation occurs within the CT band. This uncertainty is aided by the lifetime of ET, which in many

Special Issue: Paul F. Barbara Memorial Issue

Received: July 6, 2012
Revised: November 7, 2012
Published: November 9, 2012

cases is in the picosecond range, and in addition the optical spectra of excited states of the parent and product species, which are frequently overlapped and masked by other transient species, such as solvated electrons. Therefore, in such cases ultrafast optical spectra must be augmented with time-resolved X-ray absorption experiments and theoretical calculations. Such data are needed to make it possible to determine both the rates involved in the redox reaction and the mechanism responsible for electron transfer.

The number of molecules studied, to date, by these ultrafast methods is far too small to allow for a general conclusion. To that effect, we performed time-resolved optical, EXAFS, and density functional theory (DFT) studies aimed at elucidating the ET mechanism responsible for the $[Co^{III}(en)_3]^{3+}$ complex redox reaction after excitation in the LMCT band, where en stands for ethylenediamine, NH_2NH_2. The chemical properties of this coordination complex are known, including its redox reactions, and in fact, polarization and chirality studies were instrumental in understanding the nature of the structure and bonding of coordination compounds.[34] Previous photochemical studies of $[Co^{III}(en)_3]^{3+}$ complexes have shown that excitation in the ligand field, visible band, does not induce photochemistry;[31] however, excitation into the CT band by 267 nm ultrashort laser pulses, picosecond and femtosecond, induces a photoredox reaction with an electron been transferred from the ligand to the metal.[30,35] Although electron transfer is very efficient, $\Phi \sim 0.5$, it is not known if ET proceeds via an intermolecular or intramolecular mechanism.[30] Both the mechanisms of electron transfer and bond dissociation, either hemolytic or heterolytic, were not determined because, we believe, of insufficient time resolution of the photochemistry experimental systems used. To have a better understanding of the electron transfer mechanism operating in such metal–ligand complexes, we studied the redox reaction of $[Co^{III}(en)_3]Ac_3$ by means of time-resolved optical, X-ray absorption spectroscopy and DFT quantum chemical calculations. These experiments detected and measured, directly, the UV/vis absorption spectra and structures of the ground state, excited state, and transient intermediate species evolved during the course of the redox reaction. The experimental data presented here supported by theoretical calculations suggest that intramolecular electron transfer is the dominant mechanism responsible for the $[Co^{III}(en)_3]^{3+}$ to $[Co^{II}(en)_3]^{2+}$ redox reaction.

2. EXPERIMENTAL AND RESULTS

2.1. Synthesis of $[Co^{III}(en)_3]Ac_3$ and Its Absorption Spectrum. $[Co^{III}(en)_3]Ac_3$, where Ac stands for acetate, $CH_3CO_2^-$, was synthesized from $Co^{II}Ac_2{\cdot}4H_2O$ and ammonium acetate dissolved in anhydrous methanol. To this mixture was first added activated carbon, and then ethylenediamine was added dropwise, while air was bubbled through the solution. The mixture was filtered and then the methanol was removed yielding brown oil. After the removal of water, a highly water-soluble solid was derived and spectroscopic and elemental analysis confirmed that it was pure $[Co^{III}(en)_3]Ac_3$. We used the acetate ion rather than the commonly used chloride ion as the counterion of $[Co^{III}(en)_3]^{3+}$ because acetate absorbs less of the X-ray radiation used for our EXAFS studies than chloride and its higher water solubility makes it possible to prepare samples with the high concentration needed for the EXAFS experiments. The absorption spectrum of $[Co^{III}(en)_3]Ac_3$ water solution, shown in Figure 1, consists of three well-separated

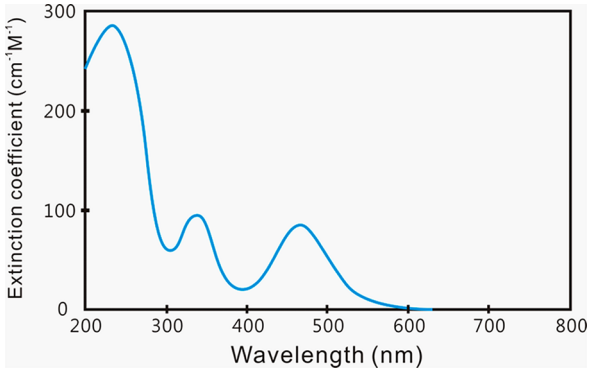

Figure 1. Absorption spectra of $[Co^{III}(en)_3]Ac_3$ in water.

bands: two bands located at ~340 and ~475 nm were assigned to ligand field bands, and the one located at ~240 nm was assigned to the charge transfer band. The excitation coefficients of $[Co^{III}(en)_3]Ac_3$ are 230, 105, and 90 cm^{-1} M^{-1} at 266, 338, and 475 nm, respectively, which are in very good agreement with the literature values.[35] It should be noted that the $[Co^{III}(en)_3]Ac_3$ CT band has much smaller extinction coefficient, ~200–300 cm^{-1} M^{-1}, than the normal value of CT bands, which is around 10^4 cm^{-1} M^{-1}, as in the case of metal oxalate complexes. The photochemical quantum yield of Co(II) was measured by the NH_4SCN indicator method and found to be ~0.50.

2.2. Femtosecond Optical Studies. The femtosecond laser system that we utilized in the studies presented here consisted of a femtosecond oscillator (Tsunami, Spectra Physics), a regenerative amplifier (Spitfire, Spectra Physics), and a multipass terawatt amplifier reported previously.[32] After amplification, the 82 MHz, 80 fs, 800 nm seeding pulses were converted to 10 Hz, 100 fs, up to 100 mJ, 800 nm output, which was split into two unequal parts 10% and 90%, which generated the optical pumping and X-ray probing pulses, respectively. The 10% beam was frequency doubled to 400 nm by a Type I BBO crystal and then passed through a wave plate and time plate for the 800 and 400 nm beams to have the same polarization and be synchronized. Subsequently, these two beams were mixed in another type I BBO crystal to yield the 100 fs, 0.3 mJ, third harmonic, 267 nm excitation beam, which was focused to a 1 mm diameter spot on the sample for excitation. The rest 800 nm beam was focused into a 5 cm quartz cell that contained a H_2O/D_2O mixture for the generation of the wide optical supercontinuum spectrum. The transient spectra were recorded on a 2D CCD as a function of the time delay between the onset of the 267 nm pump pulse and the probe continuum pulse. Samples of 0.01–0.04 M $[Co^{III}(en)_3]Ac_3$ in water were placed in a 1 mm optical path length cell and irradiated with 267 nm pulses for the measurement of the femtosecond range transient absorption spectra. The 490–790 nm broad, structureless absorption band was observed and recorded immediately after excitation. The formation of this absorption band, in the form of OD vs time (picosecond) is shown in Figure 2 from −5 ps (5 ps before excitation) to 600 ps after excitation. The maximum absorption wavelength red shifts during the first 2 ps from 565 to 725 nm, owing to the dispersion of the broad continuum probe pulse. This transient was formed within ~2 ps and decays with a two-component lifetime: the short-lived component decayed with a rate of $\sim 6 \times 10^{11}$ s^{-1}, and the long-lived component was measured to have a concentration dependent decay rate. The

dx.doi.org/10.1021/jp306706h | J. Phys. Chem. B 2013, 117, 4332–4339

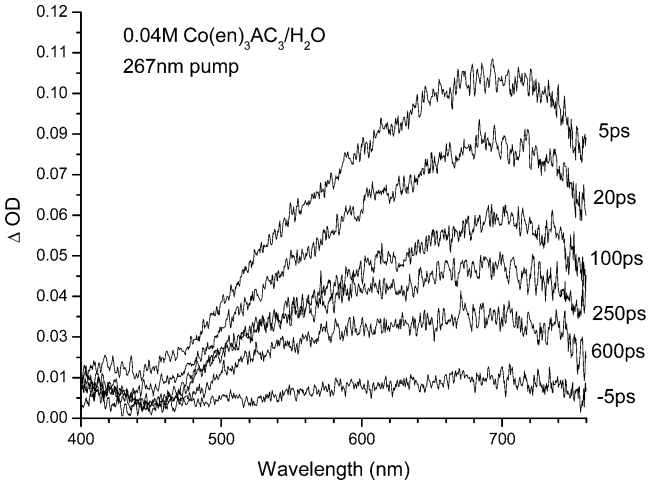

Figure 2. Transient spectra of $[Co^{III}(en)_3]Ac_3$ in water after 267 nm femtosecond excitation.

short lifetime is governed by in-cage geminate recombination, which occurs in the 10 ps range,[36,37] and the long lifetime component is controlled by the out-of-cage diffusion and concentration of the reacting components, as illustrated by reactions 2 and 3. No other transients were detected that decayed with nanosecond lifetimes. The kinetic data are listed in Table 1 and in Figure 3 in the form of normalized ΔOD, at

Table 1. Kinetics of Optical Transient Spectra of $[Co^{III}(en)_3]Ac_3$ in H_2O at Different Concentrations after 266/267 nm Excitation

concn, M	formation time τ_f, ps	decay time τ_1, ps	decay time τ_2, ps
0.04	<1	22	398
0.02	<1	22	829
0.01	<1	22	1172

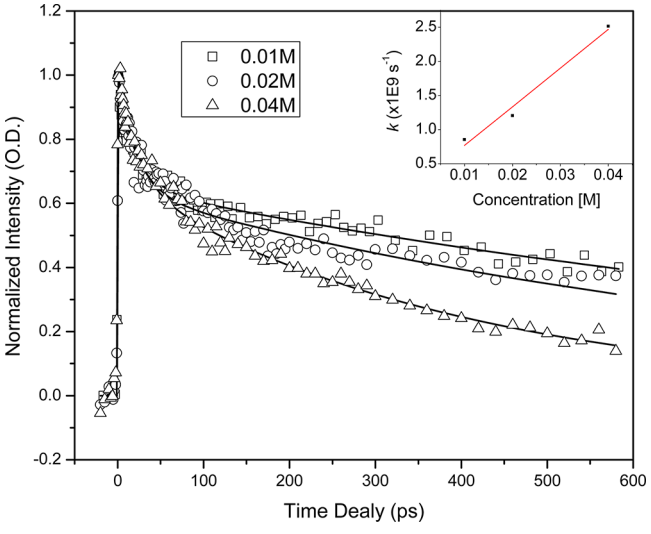

Figure 3. Time-resolved transient kinetics of $[Co^{III}(en)_3]Ac_3$ in water at various concentrations: (□) 0.01 M; (○) 0.02 M; (△) 0.04 M.

720 nm, vs delay time and the rate vs concentration (pseudo first order) is plotted in the inset of Figure 3. This 490−790 nm broad structureless transient absorption band with maximum wavelength at ∼720 nm, Figure 2, is identical with the well-known solvated electrons absorption band,[38,39] which is not surprising because metal−organo complexes dissolved in water are known to generate solvated electrons at low quantum yield.[37] The solvated electron observed in our experiments were confirmed, by linear energy dependence data, to be formed via a one photon process. We estimate that the solvated electron quantum yield generated by the $[Co^{III}(en)_3]^{3+}$ photoredox reaction was ∼0.05, or about 1 order of magnitude lower than the measured 0.5 redox quantum yield produced by the same photochemical reaction. Therefore, even though solvated electrons reduce Co(III) to Co(II), by intermolecular ET, owing to its very low quantum yield, we considered this process only as a minor ET side reaction. The three reactions that are relevant to this study and the ET mechanism are

$$[Co^{III}(en)_3]^{3+} \xrightarrow{h\nu} [Co(en)_3]^{4+} + e^-_{aq} \quad (1)$$

$$[Co(en)_3]^{4+} + e^-_{aq} \rightarrow [Co^{III}(en)_3]^{3+} \quad \text{(in-cage recombination)} \quad (2)$$

$$[Co^{III}(en)_3]^{3+} + e^-_{aq} \rightarrow [Co^{II}(en)_3]^{2+} \quad \text{(out-of-cage ET)} \quad (3)$$

We have attempted to determine the rate of electron transfer from the ethylenediamine ligand to Co(III), after photo-excitation into the 267 nm charge transfer band, by means of ultrafast optical spectroscopy. However, this procedure was proved to be not feasible because the Co(III) and Co(II) absorption bands could not be observed or be distinguished from each other owing to their overlap with the very intense solvated electron band, which is formed immediately after excitation and persists for times longer than the lifetime of the intramolecular electron transfer process. Therefore, the solvated electron absorption band masked the evolution of the cobalt complex optical transient absorption band changes. To determine the mechanism of this redox, ET, process, we performed time-resolved EXAFS experiments that measured directly the changes in the structure of the cobalt complex as a function of time after excitation. More specifically, we determined the Co−N bond length of this complex dissolved in water at 2 ps intervals between −20 ps (before excitation) and 100 ps after excitation, using 0.6 ps X-ray pulses.

2.3. Femtosecond Time-Resolved EXAFS Studies. The EXAFS experiments were performed by means of the tabletop femtosecond laser and X-ray pulsed system described previously.[19] The X-ray pulses are generated by the 90% part of the 40 mJ/pulse, 800 nm beam focused on a 0.25 mm diameter moving tungsten wire located inside a low vacuum, 10 mTorr, chamber. The laser plasma induced hard X-ray radiation exits the chamber through a 0.25 mm thick beryllium window, covered with a rolling plastic tape that protects it from the evaporated tungsten particles. The X-rays transmitted through the sample are energy dispersed by a Si(111) crystal and imaged onto the surface of a 3 cm × 3 cm liquid nitrogen cooled X-ray CCD detector. The selected energy range of the EXAFS spectrum covers from 6.5 to 8.5 keV. The pump optical pulses and probe X-ray pulses were synchronized with an accuracy of less than 2 ps using the method described previously,[40] whereas the X-ray pulse width was measured employing the Si crystal melting procedure.[41]

The Co(III) complex sample concentration for the EXAFS experiments was 1 g of $[Co^{III}(en)_3]Ac_3$ per 1 mL of H_2O, which corresponds to $\mu x \sim 1$, where μ is the X-ray mass

dx.doi.org/10.1021/jp306706h | J. Phys. Chem. B 2013, 117, 4332−4339

absorption coefficient and x is the X-ray path length through the sample. The sample was flown through a 100 μm thick by 2 mm wide stainless steel jet and circulated through a 100 mL reservoir. We estimated that each 267 nm pulse excited approximately 10% of the cobalt ethylenediamine molecules in its path through the jet, which is a negligible amount compared to the 100 mL reservoir. Yet, the reservoir sample was very often replenished. An X-ray polycapillary lens situated in front of the Be window collects the diverging X-ray beam and focuses it to a ~100 μm (fwhm) spot on the flowing jet sample, increasing the X-ray intensity at that point in the sample by a factor of 3×10^3. In this configuration the resolution of the EXAFS measurements was estimated to be 2 ps in time, 0.04 Å in bond length, and <20 eV in energy, which is limited to a large extent by the size of the X-ray lens focal spot and the distance between the X-ray lens focal spot and the detector. The Co−N bond length was determined, at various times after excitation, by accumulating 20−30 1 h EXAFS spectra, and the EXAFS data analysis was performed using the standard automated ATHENA reduction program[42] and an ab initio multiple scattering calculation program for EXAFS spectra, FEFF.[43] The EXAFS spectrum of the X-rays passing through air only was used as background for subtraction. *k-weighted* EXAFS spectra, where $k = [2m(E - E_0)/\hbar^2]^{1/2}$ (m is the mass of an electron, E_0 = 7.709 keV), were Fourier transformed over the 2−7.5 Å^{-1} range using a Kaiser−Bessel window. Subsequently, the Co−N bond length was extracted from the EXAFS μx vs energy spectra, Figure 4. We used the first shell Co−N path for

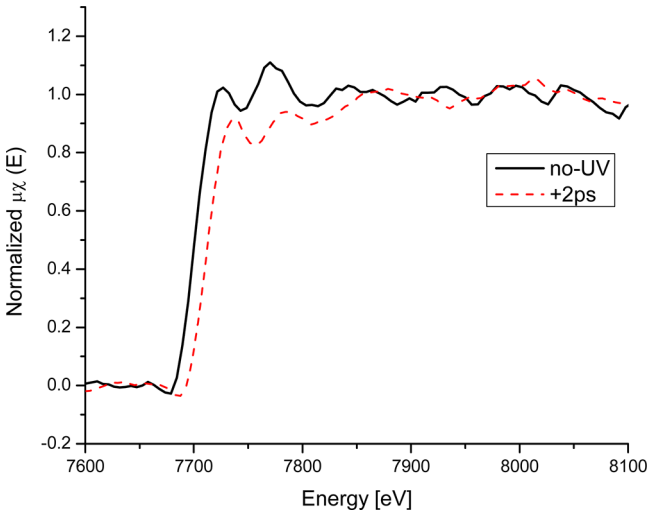

Figure 4. EXAFS spectra of $[Co^{III}(en)_3]Ac_3$ in water with (red, dotted curve) and without (black, solid curve) excitation.

phase correction, which is calculated using FEFF 8.20 on the basis of the crystalline structure of $[Co^{III}(en)_3]Cl_3$. The Co−N bond length is presented in the form of $|\chi(R)|$ vs R spectra, shown in Figure 5, which displays the bond distance between cobalt and nitrogen for the first coordination shell. Although there are discrepancies in the literature concerning the Co−N bond distances that are listed in Table 2, the bond length difference between Co^{III}−N and Co^{II}−N, $\Delta d(Co^{II}-Co^{III})$, was found to be 0.18−0.24 Å. We rely upon this 10% change in bond length to determine whether inter- or intramolecular electron transfer is the operating mechanism for the redox reaction of $[Co^{III}(en)_3]^{3+}$ complex. Essentially, the change in the Co−N bond length as a function of time determined by the

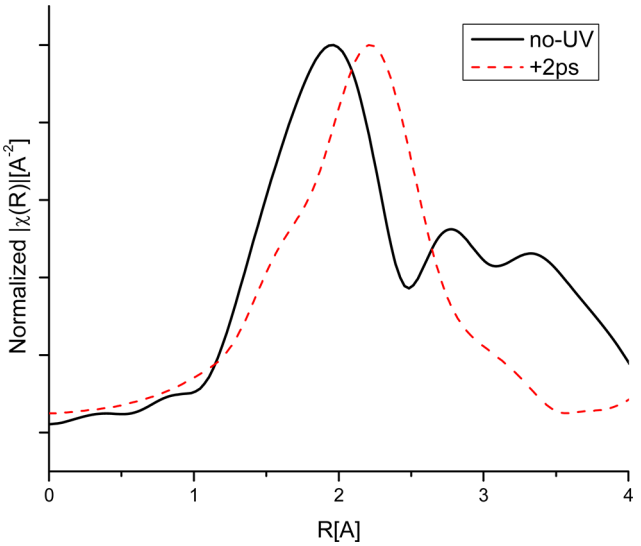

Figure 5. R space EXAFS spectra of $Co^{III}(en)_3.Ac_3$ in water recorded without UV excitation (black, solid) and with UV 2 ps after excitation (red, dotted).

Table 2. Co−N Bond Length Obtained by Time-Resolved EXAFS and Quantum Chemistry Calculations before and after 267 nm Excitation

assignment	$[Co^{III}(en)_3]^{3+}$	$[Co^{II}(en)_3]^{2+}$	$\Delta d_{Co^{II}-Co^{III}}$
exp R(Å)	1.964	2.209	0.236
cal *R* (Å) LSDA	1.95	2.13	0.18
cal *R* (Å) B3LYP	2.02	2.24	0.22
lit. *R*(Å)	1.969−1.978[50,51]	N/A	0.18−0.205[46,47a]

[a]Values for Co−N in hexaamminecobalt complexes.

EXAFS experiments form the basis for the proposed ET mechanism that reduces $[Co^{III}(en)_3]^{3+}$ to $[Co^{II}(en)_3]^{2+}$. In addition, the structures of the stable and transient species were deduced by quantum chemistry calculations using full geometry optimization for the ground state structure of the initial, and final product molecules and DFT calculation using the Gaussian 03 code[44] and the 6-31+G(d,p) basis set yielded structures that were in good agreement with the EXAFS experimental data. In addition, both the local spin density approximation (LSDA) and the Becke three-parameter hydride functional with the Lee−Yang−Purr correlation corrections (B3LYP) were also used in the DFT calculations. The structures of the ground state cobalt ethylenediamine complex derived from these calculations are listed in Table 2. The calculation of the Co−N bond length of the low spin, S = 0 $[Co^{III}(en)_3]^{3+}$ and high spin, S = 3/2 $[Co^{II}(en)_3]^{2+}$ complexes were performed starting with the known crystal structure without adding further symmetry restrictions.

3. DISCUSSION

3.1. Co−N Bond Length Changes and $[Co^{III}(en)_3]^{3+}$ Redox[45] Mechanism. The Co^{III}−N and Co^{II}−N bond lengths for hexaamminecobalt complexes have been measured and reported to have values of 1.965 and 2.170 Å, respectively.[46] Other investigators have reported that in the hexaamminecobalt complexes the Co^{III}−N bond distance is 0.18 Å shorter than the corresponding distance of the Co(II) complex.[47] Several other X-ray powder studies also find that the Co^{III}−N bond length is always shorter than the corresponding

dx.doi.org/10.1021/jp306706h | J. Phys. Chem. B 2013, 117, 4332−4339

Co^{II}–N bond length.[48,49] In this paper, the Co–N bond lengths of the $[Co^{III}(en)_3]Ac_3/H_2O$ were measured from −20 ps (20 ps before excitation) to +100 ps after excitation of the sample with 100 fs, 267 nm pulses; at times very close to excitation, data were taken at 2 ps intervals. We first determined the Co^{III}–N bond length of the molecule dissolved in water, whose literature value varies from 1.969 to 1.978 Å.[50,51] Our time-resolved EXAFS experiments measured the Co^{III}–N bond distance of the complex, at 10 ps before excitation, as 1.964 Å, which is in very good agreement with the Co^{III}–N bond distance literature value and within the 0.04 Å spatial resolution of our EXAFS system. Similar bond distance data for $[Co^{III}(en)_3]Ac_3$ were obtained using a standard continuous wave (CW) X-ray tube instrument. At time zero, $t = 0$ ps, when the optical and X-ray pulses overlap with each other inside the $[Co^{III}(en)_3]Ac_3$ flowing jet, the bond length was measured to be 2.025 Å, which corresponds to a 3% elongation of the Co–N bond. We assign the 0 ps transient to the excited $[Co^{III}(en)_3]^{3+}$ complex with a structure similar to the parent molecule within the Born–Oppenheimer approximation. At a delay time of 2 ps after excitation, analysis on the EXAFS spectra plotted in the form of bond length as a function of time, shown in Figure 6, reveal that the Co–N bond was stretched to

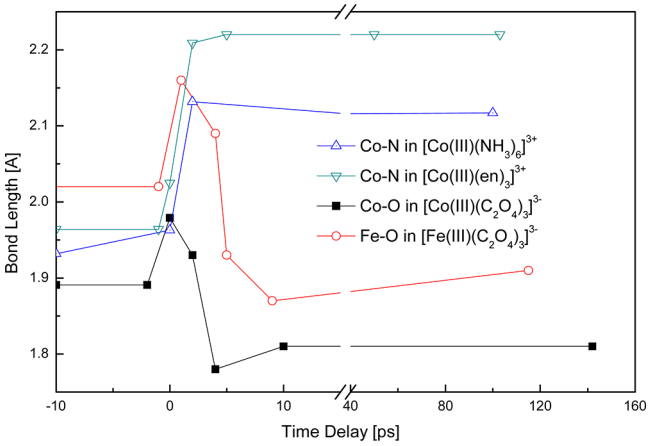

Figure 6. Metal–ligand bond lengths as a function of time after excitation: (△) Co–N bond in $[Co^{III}(NH_3)_6]^{3+}$; (▽) Co–N bond in $[Co^{III}(en)_3]^{3+}$; (■) Co–O in $[Co^{III}(C_2O_4)_3]^{3-}$; (○) Fe–O in $[Fe^{III}(C_2O_4)_3]^{3-}$.

2.209 Å and retained this value for the next 100 ps, which is the time span of the time-resolved EXAFS experiment. It is assumed, therefore, that within 2 ps after excitation, the parent molecule is transformed to a new molecule whose Co–N bond length is longer than that of the parent molecule and does not change further with time. CW EXAFS experiments revealed that the Co–N bond distance of the reduced final Co(II) product is 2.20 Å whereas the literature values of Co^{II}–N are listed as 2.115,[47] 2.5,[48,49] and 2.170 Å[46] for $[Co^{II}(NH_3)_6]^{2+}$ complexes. In addition, B3LYP/6-31+G(d,p) and LSDA calculations for the Co^{II}–N bond yielded the values of 2.236 and 2.129 Å, respectively. The difference between the calculated and experimental bond length values is 0.027 Å, which falls within the 0.04 Å spatial resolution of the experiment and 0.080 Å that is off by a factor of 2. On the basis of the good agreement of the experimental, calculated, and literature values of the Co(III) and Co(II) complexes, we assign the complex formed at 2 ps after excitation to the Co(II) complex. The experimentally determined bond distance difference between the Co(III) and Co(II) complexes determined by our EXAFS system is 0.245 Å, which is very close to the 0.18–0.205 Å[46,47] literature values. The experimentally measured change in bond length corresponds well with the theoretical calculations; therefore, all the data support our proposal that the $[Co^{III}(en)_3]^{3+}$ to $[Co^{II}(en)_3]^{2+}$ redox reaction proceeds with an intramolecular electron transfer mechanism, from the ligand to the metal, within 2 ps after illumination with 267 nm femtosecond laser pulses into the CT band.

Charge transfer excited states generally refer to excited states arising from transitions between molecular orbitals localized mainly on the metal and molecular orbital localized primarily on the ligands. These transitions effect the radial redistribution of the electronic charge between the central metal, Co in this case, and ligands, causing a change in their oxidation numbers. The electronic transition may take place from the metal to ligand, but that is a rather rare event; therefore, most likely, it involves an electron transfer from the ligand to the metal as our experimental and theoretical calculations indicate is the case for the $[Co^{III}(en)_3]^{3+}$ redox reaction, where an electron is transferred from the nitrogen molecular orbital to the molecular orbitals of the Co(III) metal that are pointing toward the nitrogen ligand. The overall redox reaction is represented by reactions 4 and 5, which show the primary intramolecular electron transfer and the dissociation reaction that follows the electron transfer process.

$$[Co^{III}(en)_3]^{3+} \xrightarrow{h\nu} [Co^{II}(en)_3]^{3+} \quad (4)$$

$$[Co^{II}(en)_3]^{3+} \rightarrow Co^{2+} + 2en + en^{+} \quad (5)$$

3.2. Intermolecular vs Intramolecular Electron Transfer Mechanism. The mechanism of electron transfer of several metal–ligand complexes of iron and cobalt excited in their CT bands have been studied by optical and X-ray ultrafast techniques, including iron and cobalt oxalate and cobalt ammonia and ethylenediamine complexes. A negligible amount of solvated electrons was formed immediately after excitation, which contributed to intermolecular electron transfer in all of these complexes; however, owing to its very low concentration and quantum yield, it was considered a minor side reaction.

$$[M^{III}(C_2O_4)_3]^{3-} \xrightarrow{h\nu} [M(C_2O_4)_3]^{3-*} \qquad (M = Co, Fe) \quad (6)$$

$$[M(C_2O_4)_3]^{3-*} \rightarrow [(C_2O_3)O - M^{III}(C_2O_4)_2]^{3-} \rightarrow [M^{III}(C_2O_4)_2]^{-} + 2CO_2^{\bullet -} \quad (7)$$

The photochemistry of Co(III) and Fe(III) oxalate complexes has been studied by many investigators[16] for several years, yet the redox mechanism was not unequivocally shown to be intermolecular and follow reactions 6 and 7 until recently,[32] even though some researchers have suggested the possibility of intramolecular electron transfer because they observed the formation of oxalate radicals during the primary photochemical process.[29,52] Revisiting the metal oxalate complex redox reaction, starting with $[Co^{III}(C_2O_4)_3]^{3+}$ and using time-resolved EXAFS, we found that the Co^{III}–O bond, which is 1.90 Å in length before irradiation, increases to 1.98 Å immediately with excitation, $t = 0$ ps; then it decreases to 1.93 Å after 2 ps and becomes even shorter, 1.78 Å, after 4 ps. The 4 ps transient was

dx.doi.org/10.1021/jp306706h | J. Phys. Chem. B 2013, 117, 4332–4339

attributed to the Co(III) complex after bond dissociation. Five picoseconds after excitation, the Co−O bond length was measured to be 1.81 Å and remained at this value for 142 ps.[32] The bond distance changes observed between 4 and 142 ps after excitation were attributed to Co^{III}−O bond dissociation and the formation of CO_2^- ions before significant electron transfer occurred. Subsequently, the CO_2^- donated an electron to the Co(III) complex initiating its reduction to the Co(II) complex with a Co^{II}−O bond length of 2.209 Å. Therefore, the Co(III) to Co(II) redox reaction was visualized as proceeding via intermolecular electron transfer, even though the molecule was excited in the charge transfer band. The Fe−O bond distance changes as a function of time after excitation for Fe(III) oxalate complex followed a similar path as the Co(III) oxalate complex and consequently its redox mechanism was also assigned to intermolecular electron transfer. The metal to ligand bond length at various times after excitation, for both Fe(III) and Co(III) oxalate complexes, is depicted in Figure 6.

In contrast, when Co(III) ammonia complexes were excited in the CT band, the Co−N bond length was elongated by ∼0.2 Å within 2 ps and retained the same bond length value for the 140 ps time duration of these experiments. This bond length is exactly the same as the Co^{II}−N bond length; therefore, the Co(III) to Co(II) redox reaction was assigned to intramolecular electron transfer. The experimental data obtained for the $[Co^{III}(en)_3]^{3+}$ complex presented in this article follow the Co(III) ammonia complex ET behavior, where the Co−N bond length increased from 1.963 to 2.209 Å within 2 ps and remained as such for at least 100 ps after excitation. The Co−N bond length observed at 2 ps after excitation has essentially the same Co−N bond length as the reduced Co(II) complex; therefore, the photoinduced redox operating mechanism in both of these complexes is proposed to be intramolecular electron transfer. It is important to note the fact that even though all the Fe and Co complexes studied and discussed in this article were excited in the CT band and the photoinduced redox reaction proceeds with a similar high redox quantum yield, the dominant ET operating mechanism differs; in some cases it is intramolecular whereas in others it is found to be intermolecular. The reason for the very different operating mechanisms may be quite complicated and not due to a single source. Here we propose some of the likely possibilities from the point of view of the ligand and counterion effects.

Comparing the four molecules in Figure 6, it is difficult to draw a conclusion from the influence of the central metals. However, there are some common characteristics that may be derived from the amine ligands. (a) Electron donor effect: Both the ammonia and ethylenediamine groups are stronger electron donors than the oxalate group, whereas nitrogen has more electron lone pairs and smaller electronegativity than oxygen. These facts suggest that NH_3 and ethylenediamine metal complexes would favor intramolecular ET. (b) Steric effect: For efficient intramolecular ET, it is rather mandatory that the electron donor group, i.e., ligand, be at the proper orientation with the acceptor, metal, or that the donor group be free to rotate and achieve the needed orientation within a few picoseconds, without hindrance from other groups of the molecule. Such freedom of alignment favors intramolecular electron transfer and consequently the reduction of the metal, M, from M(III) to M(II) within several picoseconds. This we believe is the case for the $[Co^{III}(NH_3)_6]^{3+}$ and $[Co^{III}(en)_3]^{3+}$ complexes. However, in the case of the M(III) oxalate and M(II) oxalate, intramolecular ET will require the oxalate donor group to perform in-plane or out-of-plane movement(s) that may strain the M−O bond, leading to bond dissociation before electron transfer can occur. In contrast to NH_3 and ethylenediamine metal complexes, this suggests that in metal oxalate complexes intermolecular electron transfer is highly possible. It should also be noted that the interaction between the positively charged metal ion and negatively charged oxalate ligand is much stronger than that between metal and the neutral amine ligand due to the electrostatic forces. Therefore, it is highly improbable for the M(III) oxalate configuration to survive a realignment potential force induced by the excitation, which means that it will be rather difficult for the ligand group to reorient. We are studying this type of steric effects, and preliminary data suggest that this is a possible cause for the observed dissociation and subsequent intermolecular electron transfer in Fe(III) oxalate complexes. However, we prefer, at this time, to offer the steric effect as a tentative explanation for the ET mechanism where not the size of the ligand but the ligand orientation degree of freedom plays an important role in electron transfer.

When the concentration of the counterion increases, acetate in this case, or chloride in the more common complexes, the possibility arises of ion pair $[Co^{III}(en)_3]^{3+}Ac^-_3$ formation. In such a case, electron transfer quite possibly might take place between the acetate ion and cobalt metal. If the ion pair is considered a two-molecule entity, the electron transfer will be intermolecular. In this case if the ion pair is considered one molecule, then the ET mechanism will be intramolecular. One means for distinguishing between the ion complex and ion pair is the concentration of the anion. We have not observe any change in the electron transfer rate with concentration, although it is possible that the 2 ps time resolution of our experiments is not sufficient to resolve the difference in electron transfer from the nitrogen, or the acetate ion to the central cobalt atom. However, it will be arbitrary to assume that the intramolecular ET happens between the metal and nitrogen or amine group, but not between metal and the counterion, acetate, in this case. It is noted that in metal oxalate complexes, the counterion is a positive ion, for example, NH_4^+ or K^+, and it is not expected to donate an electron to the metal−ligand group. Therefore, for metal oxalate complexes, intramolecular ET is expected to occur within the metal−ligand group, but not within ion pairs. The proposal of "counter ion electron donor accelerates the intramolecular electron transfer" should be examined by especially designed experiments.

Regarding the spin changes taking place during the intramolecular ET it should be noted that it is generally accepted that a spin change transition is forbidden in small molecules; however, for large complexes, the spin forbidden transition may occur due to spin−orbit coupling. In the case of the cobalt amine complex, the spin of cobalt changes from $S = 0$ to $S = 3/2$.

4. CONCLUSION

Histograms of bond length changes, transient optical spectra, and kinetics have been obtained by means of ultrafast time-resolved EXAFS and optical experiments that are further supported by the close agreement with theoretical calculations. On the basis of these data, we propose that the mechanism responsible for the photo redox reaction of $[Co^{III}(en)_3]^{3+}$ to $[Co^{II}(en)_3]^{2+}$ after femtosecond excitation in the CT band is intramolecular ET.

dx.doi.org/10.1021/jp306706h | J. Phys. Chem. B 2013, 117, 4332−4339

By comparing four different metal−ligand complexes and without further in depth knowledge of the molecular-group motion, group orientation, and counterion effect, we find that, at the present time, it is rather difficult to predict, a priori, the ET mechanism of such a molecule. Our experimental data suggest that ligand to metal charge transfer does not automatically lead to an intramolecular ligand to metal electron transfer reaction path; i.e., CT is not always the same as ET, which one may normally assume.

AUTHOR INFORMATION

Corresponding Author

*E-mail: J.C., jiec@sjtu.edu.cn; P.M.R., pmrentze@uci.edu.

Notes

The authors declare no competing financial interest.

ACKNOWLEDGMENTS

This research was supported in part by the W. M. Keck Foundation. J.C. thanks the National Natural Science Foundation of China under Grants Nos. 61222509 and 11121504. We also thank Dr. Xiao-Yu Cao for preparing the $[Co^{III}(en)_3]Ac_3$ samples.

REFERENCES

(1) Taube, H.; Myers, H.; Rich, R. L. *J. Am. Chem. Soc.* **1953**, *75*, 4118−4119.

(2) Hush, N. S.; Vlcek, A. A.; Stranks, D. R.; Marcus, R. A.; Weiss, J.; Bell, R. P.; Halpern, J.; Orgel, L. E.; Adamson, A. W.; Dainton, F. S.; et al. *Discuss. Faraday Soc.* **1960**, *29*, 113−136.

(3) Marcus, R. A. *Annu. Rev. Phys. Chem.* **1964**, *15*, 155−196.

(4) Richardson, D. E.; Taube, H. *Coord. Chem. Rev.* **1984**, *60*, 107−129.

(5) Marcus, R. A.; Sutin, N. *Biochim. Biophys. Acta* **1985**, *811*, 265−322.

(6) Closs, G. L.; Calcaterra, L. T.; Green, N. J.; Penfield, K. W.; Miller, J. R. *J. Phys. Chem. A* **1986**, *90*, 3673−3683.

(7) Bixon, M.; Jortner, J. Electron transfer - from isolated molecules to biomolecules. In *Advances in Chemical Physics: Electron Transfer - from Isolated Molecules to Biomolecules. Part 1*; Prigogine, I., Rice, S. A., Eds.; John Wiley & Sons: New York, 1999; Vol. *106*, pp 35−202.

(8) Gawelda, W.; Johnson, M.; de Groot, F. M. F.; Abela, R.; Bressler, C.; Chergui, M. *J. Am. Chem. Soc.* **2006**, *128*, 5001−5009.

(9) Campagna, S.; Puntoriero, F.; Nastasi, F.; Bergamini, G.; Balzani, V. Photochemistry and photophysics of coordination compounds: Ruthenium. In *Photochemistry and Photophysics of Coordination Compounds I*; Balzani, V., Campagna, S., Eds.; Springer-Verlag Berlin: Berlin, 2007; Vol. *280*, pp 117−214.

(10) Solomon, E. I.; Xie, X. J.; Dey, A. *Chem. Soc. Rev.* **2008**, *37*, 623−638.

(11) Miller, J. S.; Min, K. S. *Angew. Chem.-Int. Ed.* **2009**, *48*, 262−272.

(12) Zhang, X.; Smolentsev, G.; Guo, J.; Attenkofer, K.; Kurtz, C.; Jennings, G.; Lockard, J. V.; Stickrath, A. B.; Chen, L. X. *J. Phys. Chem. Lett.* **2011**, *2*, 628−632.

(13) Van Kuiken, B. E.; Huse, N.; Cho, H.; Strader, M. L.; Lynch, M. S.; Schoenlein, R. W.; Khalil, M. *J. Phys. Chem. Lett.* **2012**, *3*, 1695−1700.

(14) Sato, T.; Nozawa, S.; Tomita, A.; Hoshino, M.; Koshihara, S.-y.; Fujii, H.; Adachi, S.-i. *J. Phys. Chem. C* **2012**, *116*, 14232−14236.

(15) Closs, G. L.; Miller, J. R. *Science* **1988**, *240*, 440−447.

(16) Stufkens, D. J.; Vlcek, A. *Coord. Chem. Rev.* **1998**, *177*, 127−179.

(17) Ciofini, I.; Laine, P. P.; Bedioui, F.; Adamo, C. *J. Am. Chem. Soc.* **2004**, *126*, 10763−10777.

(18) Solomon, E. I.; Sundaram, U. M.; Machonkin, T. E. *Chem. Rev.* **1996**, *96*, 2563−2605.

(19) Bredas, J. L.; Beljonne, D.; Coropceanu, V.; Cornil, J. *Chem. Rev.* **2004**, *104*, 4971−5003.

(20) Chen, L. X.; Jäger, W. J. H.; Jennings, G.; Gosztola, D. J.; Munkholm, A.; Hessler, J. P. *Science* **2001**, *292*, 262−264.

(21) Bressler, C.; Milne, C.; Pham, V.-T.; ElNahhas, A.; van der Veen, R. M.; Gawelda, W.; Johnson, S.; Beaud, P.; Grolimund, D.; Kaiser, M.; et al. *Science* **2009**, *323*, 489−492.

(22) Lorenc, M.; Hébert, J.; Moisan, N.; Trzop, E.; Servol, M.; Buron-Le Cointe, M.; Cailleau, H.; Boillot, M. L.; Pontecorvo, E.; Wulff, M.; et al. *Phys. Rev. Lett.* **2009**, *103*, 028301.

(23) Nozawa, S.; Sato, T.; Chollet, M.; Ichiyanagi, K.; Tomita, A.; Fujii, H.; Adachi, S.-i.; Koshihara, S.-y. *J. Am. Chem. Soc.* **2009**, *132*, 61−63.

(24) Huse, N.; Kim, T. K.; Jamula, L.; McCusker, J. K.; de Groot, F. M. F.; Schoenlein, R. W. *J. Am. Chem. Soc.* **2010**, *132*, 6809−6816.

(25) Khalil, M.; Marcus, M. A.; Smeigh, A. L.; McCusker, J. K.; Chong, H. H. W.; Schoenlein, R. W. *J. Phys. Chem. A* **2005**, *110*, 38−44.

(26) Chen, L. X.; Zhang, X.; Wasinger, E. C.; Lockard, J. V.; Stickrath, A. B.; Mara, M. W.; Attenkofer, K.; Jennings, G.; Smolentsev, G.; Soldatov, A. *Chem. Sci.* **2010**, *1*, 642−650.

(27) Huse, N.; Cho, H.; Hong, K.; Jamula, L.; de Groot, F. M. F.; Kim, T. K.; McCusker, J. K.; Schoenlein, R. W. *J. Phys. Chem. Lett.* **2011**, *2*, 880−884.

(28) Van Kuiken, B. E.; Khalil, M. *J. Phys. Chem. A* **2011**, *115*, 10749−10761.

(29) Copestake, T. B.; Uri, N. *Proc. R. Soc. London, Math. Phys. Sci.* **1955**, *228*, 252−263.

(30) Klein, D.; Moeller, C. W. *Inorg. Chem.* **1965**, *4*, 394−398.

(31) Balzani, V.; Carassiti, V. *Photochemistry of Coordination Compounds*; Academic: New York, 1970.

(32) Chen, J.; Zhang, H.; Tomov, I. V.; Ding, X.; Rentzepis, P. M. *Proc. Natl. Acad. Sci. U. S. A.* **2008**, *105*, 15235−15240.

(33) Chen, J.; Zhang, H.; Rentzepis, P. M. *J. Phys. Chem. A* **2010**, *114*, 2751−2756.

(34) Broomhead, J. A.; Dwyer, F. P.; Hogarth, J. W.; Sievers, R. E. Resolution of the Tris(Ethylenediamine)Cobalt(III) Ion. In *Inorganic Syntheses*; Rochow, E. G., Ed.; John Wiley & Sons: New York, 1960; Vol. *6*, pp 183−186.

(35) Balzani, V.; Moggl, L.; Scandola, F.; Carassiti, V. *Inorg. Chim. Acta Rev.* **1967**, *1*, 7−34.

(36) Crowell, R. A.; Lian, R.; Shkrob, I. A.; Bartels, D. M.; Chen, X. Y.; Bradforth, S. E. *J. Chem. Phys.* **2004**, *120*, 11712−11725.

(37) Zhang, H.; Chen, J.; Tomov, I. V.; Dvornikov, A. S.; Rentzepis, P. M. *J. Phys. Chem. A* **2007**, *111*, 11584−11588.

(38) Baxendale, J. H.; Capellos, C.; Land, E. J.; Keene, J. P.; Ebert, M.; Swallow, A. J.; Davies, J. V.; Francis, J. M.; Gilbert, C. W.; Fielden, E. M.; et al. *Nature* **1964**, *201*, 468−470.

(39) Pommeret, S.; Naskrecki, R.; van der Meulen, P.; Menard, M.; Vigneron, G.; Gustavsson, T. *Chem. Phys. Lett.* **1998**, *288*, 833−840.

(40) Chen, J.; Zhang, H.; Tomov, I. V.; Ding, X. L.; Rentzepis, P. M. *Chem. Phys. Lett.* **2007**, *437*, 50−55.

(41) Tomov, I. V.; Chen, J.; Ding, X.; Rentzepis, P. M. *Chem. Phys. Lett.* **2004**, *389*, 363−366.

(42) Ravel, B.; Newville, M. *J. Synchrotron Radiat.* **2005**, *12*, 537−541.

(43) Ankudinov, A. L.; Bouldin, C. E.; Rehr, J. J.; Sims, J.; Hung, H. *Phys. Rev. B* **2002**, *65*, 104107.

(44) Frisch, M. J.; Trucks, G. W.; Schlegel, H. B.; Scuseria, G. E.; Rob, M. A.; Cheeseman, J. R.; Jr., J. A. M.; Vreven, T.; Kudin, K. N.; Burant, J. C.; et al. *Gaussian 03*; Gaussian, Inc.: Wallingford, CT, 2003.

(45) Beattie, J. K.; Moore, C. J. *Inorg. Chem.* **1982**, *21*, 1292−1295.

(46) Newman, J. M.; Binns, M.; Hambley, T. W.; Freeman, H. C. *Inorg. Chem.* **1991**, *30*, 3499−3502.

(47) Kime, N. E.; Ibers, J. A. *Acta Crystallogr. B* **1969**, *25*, 168−169.

(48) Basolo, F.; Pearson, R. G. *Mechanisms of Inorganic Reactions*, 1st ed.; John Wiley & Son: New York, 1967.

(49) Emeleus, H. J.; Anderson, J. S. *Modern Aspects of Inorganic Chemistry*, 3rd ed.; D. Van Nostrand: Princeton, NJ, 1960.

(50) Iwata, M.; Nakatzu, K.; Saito, Y. *Acta Crystallogr. B* **1969**, *25*, 2562−2571.

(51) Makotchenko, E.; Baidina, I.; Naumov, D. *J. Struct. Chem.* **2006**, *47*, 499−503.
(52) Pozdnyakov, I. P.; Kel, O. V.; Plyusnin, V. F.; Grivin, V. P.; Bazhin, N. M. *J. Phys. Chem. A* **2008**, *112*, 8316−8322.